Number 3 Volume 16 September 2010 Journal of Engineering

ANALYSIS OF CONCRETE FLEXURAL MEMBERS REINFORCED WITH FIBRE POLYMER

Asst. Prof. Dr. Nazar K. Oukaili, Ahlam Ali Al-Asadi
Civil Engineering Department, College of Engineering, University of Baghdad

ABSTRACT:

Analytical model is used in this paper to predict the load carrying capacity of structural concrete members under flexural and normal force which can be concentric or eccentric. The analysis is based on requirement of equilibrium and compatibility of strain in concrete and steel or FRP. The adopted model is based on the real stress - strain diagrams for materials. In accordance with this model, the member cross section is covered by a mesh with the smallest cells. After that, stress or strain is determined in each cell and the integral is substituted by the process of summation to define the elements of stiffness matrix. The force vectors equations have nonlinear behaviour. However, in this model, these nonlinear equations are changed to linear equations using the iteration methods with fixity of secant modulus of elasticity in each iteration cycle. In this paper, FORTRAN computer program language is used to compute the force and strains vectors. The comparison between the analytical results obtained from the used model and experimental data for other researchers is performed. The analytical model is giving a reasonable agreement between the theoretical and experimental results.

تحليل الأعضاء الخرسانية المنحنية المسلحة بالألياف البوليميرية

الخلاصة:

في هذه الورقة البحثية تم أقتراح أنموذج تحليلي لتحديد السعة الحملية لعناصر الخرسانية الأنشائية المعرضة للأنحناء والقوة المحورية مركزية اوغيرمركزية. ان طبيعة التحليل تعتمد على شروط الأتزان والتوافق في الأنفعالات في الخرسانة والحديد. يستند الأنموذج المستخدم على المخططات البيانية الحقيقية الكاملة لتشوه الخرسانة والحديد. ان أسلوب الحل وفقآ للأنموذج المقترح يعتمد بشكل أساسي على تغطية المقطع العرضي بشبكة ذات خلايا صغيرة جداً. بعد ذلك يؤخذ متوسط الأجهادات اوالأنفعالات في حدود كل خلية وبالتالي يتم الأنتقال من التكامل التفاضلي الى المجموع التكاملي لتحديد عناصر مصفوفة صلادة المقطع. من جهة أخرى، فان المعادلات الرئيسية لمتجهات القوى لها صفة لا خطية، الا أنه يتم في النموذج المدروس تحويل المعادلات اللاخطية الى معادلات خطية باستخدام الطرق التكرارية مع تثبيت معامل المرونة القاطعي خلال كل دورة تكرار. في هذه الورقة البحثية استخدم برنامج بلغة فورتران لتحديد متجهة القوى والانفعالات الخطية. تمت مقارنة النتائج المستحصلة من هذا الأنموذج مع النتائج المختبرية لعدد من الباحثين. ولوحظ ان الأنموذج التحليلي يعطي توافق معقول بين النتائج النظرية والمختبرية.

KEYWORDS: Flexural Member, Fibre Reinforced Polymer, Ultimate Moment Capacity, Moment-Curvature diagram

INTRODUCTION

Conventional concrete structures are reinforced with nonprestressed and/or prestressed steel. The steel is initially protected against corrosion by the alkalinity of the concrete, usually resulting in durable and serviceable construction. For many structures subjected to aggressive environments,

such as marine structures, bridges and parking garages exposed to deicing salts, combinations of moisture, temperature and chlorides reduce the alkalinity of the concrete and result in the corrosion of reinforcing and prestressing steel. The corrosion process ultimately causes concrete deterioration and loss of serviceability. To address corrosion problems, professionals have turned to alternative metallic reinforcement, such as epoxy-coated steel bars. While effective in some situations, such remedies may still be unable to completely eliminate the problems of steel corrosion (cited in ACI 440H, 2000).

Recently, composite materials made of fibres embedded in a polymeric resin, also known as fibre-reinforced polymers (FRP), have become an alternative to steel reinforcement for concrete structures. Because FRP materials are nonmagnetic and non-corrosive, the problems of electromagnetic interference and steel corrosion can be avoided with FRP reinforcement. Additionally, FRP materials exhibit several properties, such as high tensile strength, that make them suitable for use as structural reinforcement (Dolan et al., 1999).

STRESS-STRAIN MODEL FOR MATERIALS

In 1986, Korpenko (Korpenko et al., 1986) suggested a relationship to predict the stress-strain diagram for concrete and steel under unaxial loads. This relationship unified the stress-strain diagram represented for concrete in tension or compression and all types of steel (mild or high strength steel).

Let:

$$\tilde{\sigma}_m = \left|\frac{\sigma_m}{\hat{\sigma}_m}\right| \quad ; \quad \tilde{\varepsilon}_m = \left|\frac{\varepsilon_m}{\hat{\varepsilon}_m}\right| \tag{1}$$

where:

$\tilde{\sigma}_m$, $\tilde{\varepsilon}_m$: relative level of stress and strain, respectively; $\hat{\sigma}_m$, $\hat{\varepsilon}_m$: stress and strain at the peak of stress-strain diagrams for materials (concrete and steel); σ_m , ε_m: stress and strain for materials (concrete or steel); m: represents the parameters for concrete and steel, ($m = c, t$: represents the compression or tension in concrete, respectively. $m = s, ps, f$: represents the nonprestressing, prestressing steel or fibre reinforced polymer, respectively).

The nonlinear behaviour of the stress-strain diagram for materials (concrete or steel) can be represented by the following expression (Korpenko et al., 1986):

$$\sigma_m = \varepsilon_m E_m \nu_m \tag{2}$$

where:

E_m: initial modulus of elasticity for material (concrete or steel); ν_m: coefficient of elastic strain (represents the elastic strain to the total strain) (Korpenko et al., 1986).

$$\begin{aligned} &\nu_m = 1, && |\sigma_m| \le |\sigma_{m,el}| \\ &\nu_m = \hat{\nu}_m \pm (\nu_o - \hat{\nu}_m)\sqrt{1 - e_{1m}\eta_m - e_{2m}\eta_m^2}, && |\sigma_m| > |\sigma_{m,el}| \end{aligned} \tag{3}$$

Where (Korpenko et al., 1986):

$$\eta_m = \frac{\sigma_m - \sigma_{m,el}}{\hat{\sigma}_m - \sigma_{m,el}} = \frac{\tilde{\sigma}_m - \sigma_{m,el}}{1 - \tilde{\sigma}_{m,el}} \le 1 \tag{4}$$

where:
$\sigma_{m,el}$: proportional limit of material; $\tilde{\sigma}_{m,el}$: relative level of proportional limit of material; $\hat{v}_m$: coefficient of elastic strain when the stress σ_m reaches the ultimate stress $\hat{\sigma}_m$; v_o: coefficient depended on relative level stress for material; e_{1m}, e_{2m}: coefficient depending on type of material (steel or concrete).

$$e_{2m} = 1 - e_{1m} \quad (5)$$

To use Eq.(3), the e_{1m} must be less than 2 (Korpenko et al., 1986).

Stress-Strain Model for Concrete

The stress-strain diagram of concrete (Fig.1) is represented using Eq.(2) and Eq.(3) by taking the following expressions for coefficient v_m and e_{1c} (Korpenko et al., 1986):

$$\begin{aligned} v_o &= 1 \quad ; \quad \tilde{\varepsilon}_c \le 1 \\ v_o &= 2.05\,\hat{v}_c \quad ; \quad \tilde{\varepsilon}_c > 1 \end{aligned} \quad (6)$$

$$\begin{aligned} e_{1c} &= 1.72 - 1.82\,\hat{v}_c \quad ; \quad \tilde{\varepsilon}_c \le 1 \\ e_{1c} &= 1.95\,\hat{v}_c - 0.138 \quad ; \quad \tilde{\varepsilon}_c > 1 \end{aligned} \quad (7)$$

where:
$\hat{\sigma}_c$: stress at the peak of stress-strain diagram for concrete; $\hat{\varepsilon}_c$: strain at the peak of stress-strain diagram for concrete; $\hat{v}_c$: coefficient of elastic strain when $\sigma_c = \hat{\sigma}_c$; E_c: initial modulus of elasticity for concrete; v_o: coefficient that depends on the stress level of concrete; e_{1c}: coefficient that depends on type of materials.

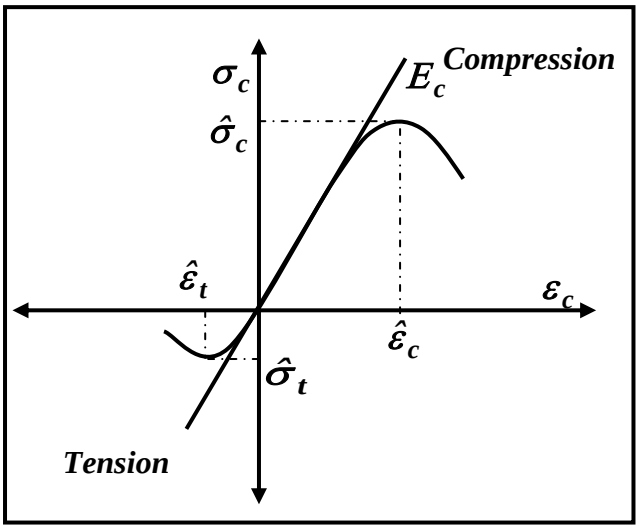

Figure 1: Stress-strain diagram for concrete (Oukaili, 1998)

Stress-Strain Model for Steel

In addition to the general mechanical properties in concrete and steel which are required to simulate the $\sigma - \varepsilon$ diagram; steel has special mechanical characteristics such as yield stress σ_y or $\sigma_{0.2}$ and yield strain $\varepsilon_{0.2}$ and coefficient of elastic strain $\nu_{0.2}$.

The elastic stress for high strength steel (Fig.2a) is determined by:

$$\sigma_{s,el} = \beta_{el}\ \sigma_{0.2} \tag{8}$$

Where:
$\sigma_{0.2}$: stress for steel at yield state; β_{el}: coefficient that depends on steel type.
The coefficient e_{1s} can be found from equation below (Korpenko et al., 1986):

$$e_{1s} = \frac{(v_o - \hat{v}_s)^2(\eta_{0.2}^2 - 1) + (v_{0.2} + \hat{v}_2)^2}{(\eta_{0.2}^2 - \eta_{0.2})(1 - \hat{v}_s)^2} \le 2 \tag{9}$$

In mild steel the linear branch until proportional limit is determined using Eq.(2) with taking $v_s = 1$.

When the stress-strain diagram for mild steel is represented, the yield plateau is observed (see Fig.2a). In this Figure $\hat{\sigma}_s$, $\hat{\varepsilon}_s$ represent the stress and strain in the end yield plateau, and determined as follows (Korpenko et al., 1986):

$$\hat{\sigma}_s = (1.01 : 1.03)\sigma_y \quad ; \quad \hat{\varepsilon}_s = \frac{\hat{\sigma}_s}{E_s} + \lambda_y \quad ; \quad \sigma_{0.2} = 0.99\,\sigma_y \tag{10}$$

where:
λ_y: length of yield plateau depends on steel type (0.008-0.015).

After the yield point, mild steel will undergo a period of strain hardening, in which the stress slowly increases with a rapid increasing of strain up to rupture. The strain hardening region is represented using Eq.2; Eq.3; and Eq.9, with taking: point c to complete the strain hardening diagram (Fig.2b), its coordinate is (Korpenko et al., 1986):

$$\sigma_{s(c)} \approx 1.2\,\sigma_y \quad ; \quad \varepsilon_{s(c)} = 0.05 + \frac{\sigma_{s(c)}}{E_s} \tag{11}$$

With taking:

$$\eta_{s(c)} = \frac{\sigma_{s(c)} - \hat{\sigma}_s}{\dot{\sigma}_s - \hat{\sigma}_s} \quad ; \quad v_{s(c)} = \frac{\sigma_{s(c)}}{E_s \varepsilon_{s(c)}} \tag{12}$$

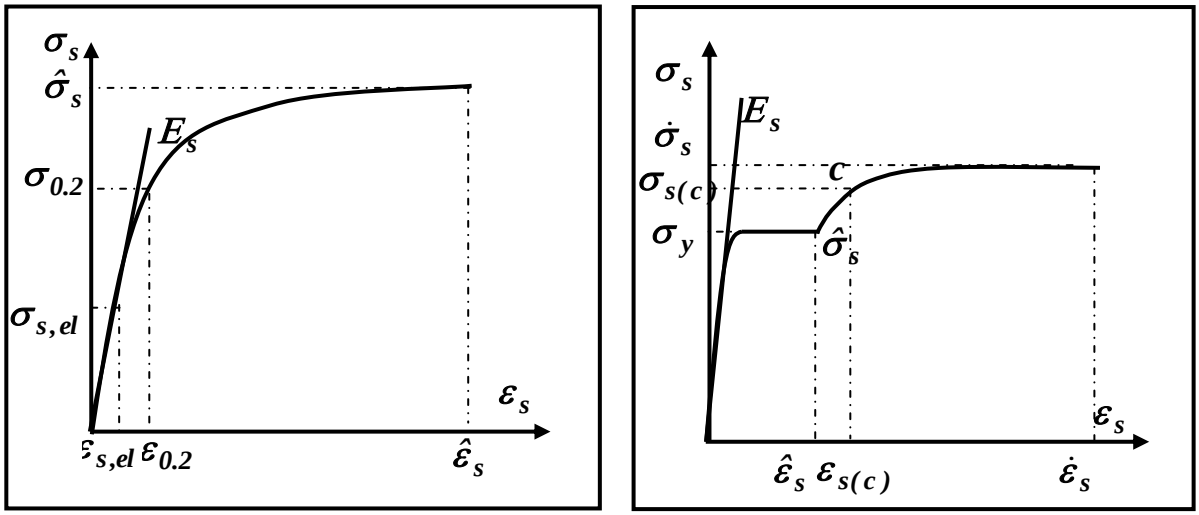

(a) **(b)**

Figure 2: Stress-strain diagrams for (a) mild steel, (b) high strength steel (Oukaili, 1998)

Fibre Reinforced Polymer (FRP) Model

For FRP materials, an ideal elastic behaviour is assumed until the failure **(Pešić and Pilakoutas**, 2005) (Fig.3) and the unaxial tensile stress-strain ($\sigma_f - \varepsilon_f$) relation is simply given by:

$$\sigma_f = E_f \varepsilon_f \quad , \quad 0 \le \varepsilon_f \le \varepsilon_{fu} \tag{13}$$

where:
E_f : elastic modulus for FRP; ε_f : strain for FRP; ε_{fu} : strain at rupture.

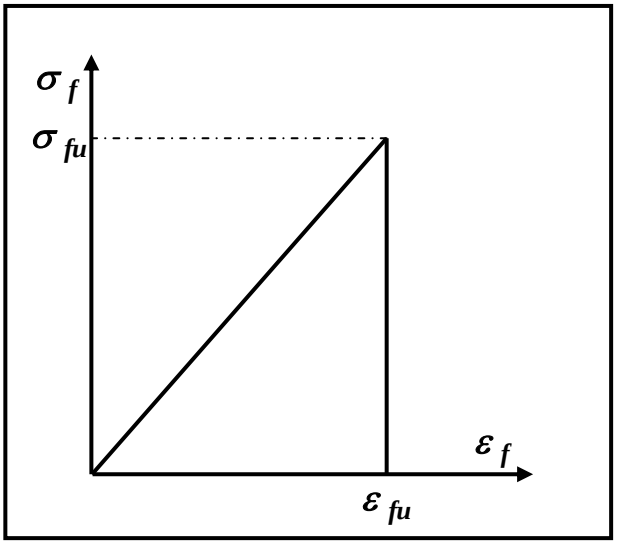

Figure 3: Stress-strain diagrams for FRP (Pešić and Pilakoutas, 2005)

COMPARISON BETWEEN KORPENKO MODELS WITH EXPERIMENTAL RESULTS FOR CONCRETE

The analysis and design of structural concrete depend on the prediction of stress-strain relationship for concrete in compression. According to that, there is a mathematical model in the present study to predict the stress-strain diagram for concrete under unaxial load. It is compared with actual experimental data which are collected from the following works: Wang et al., 1978; Nilson et al., 1986; and Tasnimi, 2004. These data are classified into three groups according to strength: low strength concrete (LSC), normal strength concrete (NSC), and high strength concrete (HSC). Fig.4 illustrates detailing comparison between of Korpenko´s stress-strain relationship and the experimental data for the LSC, NSC, and HSC and the comparison between the analytical and experimental data shows good agreement.

COMPARISON BETWEEN KORPENKO MODELS WITH EXPERIMENTAL RESULTS FOR STEEL

Korpenko´s analytical steel model for mild and high strength steel is compared with experimental data. In mild steel the experimental data collected from the following studies: Goto et al., 1998; and Cho et al., 2004, while the experimental data for high strength steel collected from: Leax et al and Canfield, 2005. The Fig.5 demonstrates these comparisons and a good agreement between the analytical and experimental results can be observed.

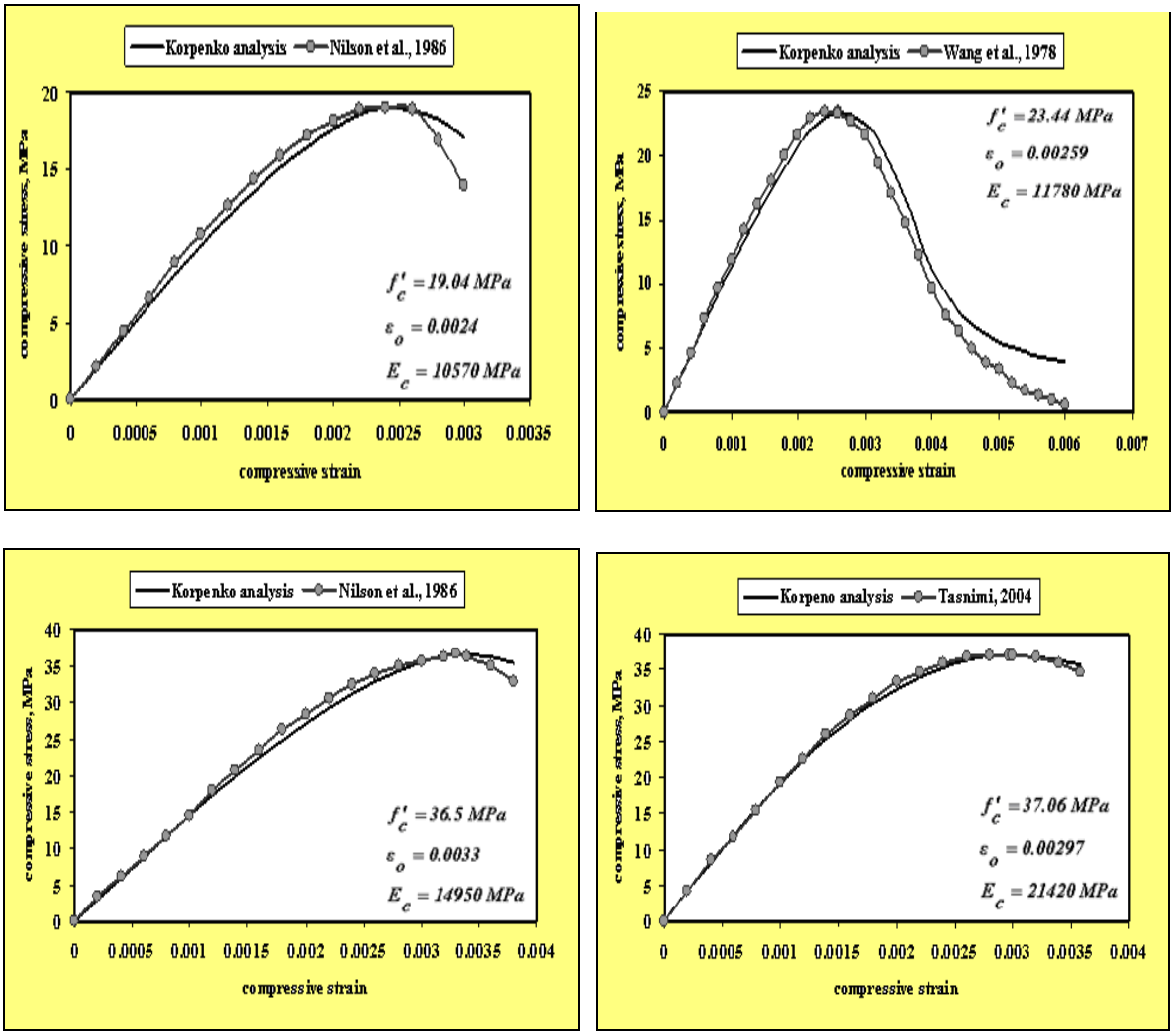

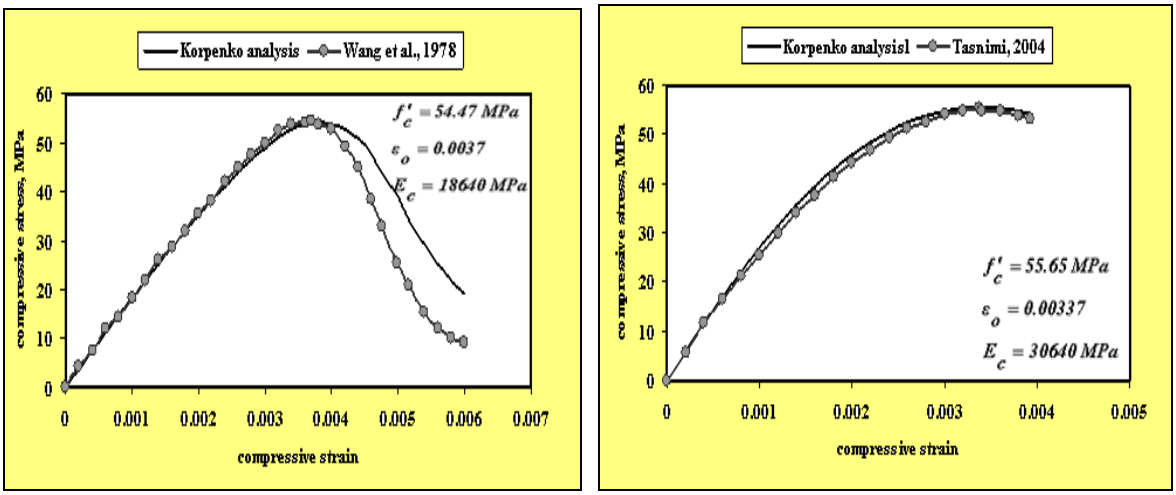

Figure 4: Comparison of proposed model with experimental data to LSC, NSC, HSC

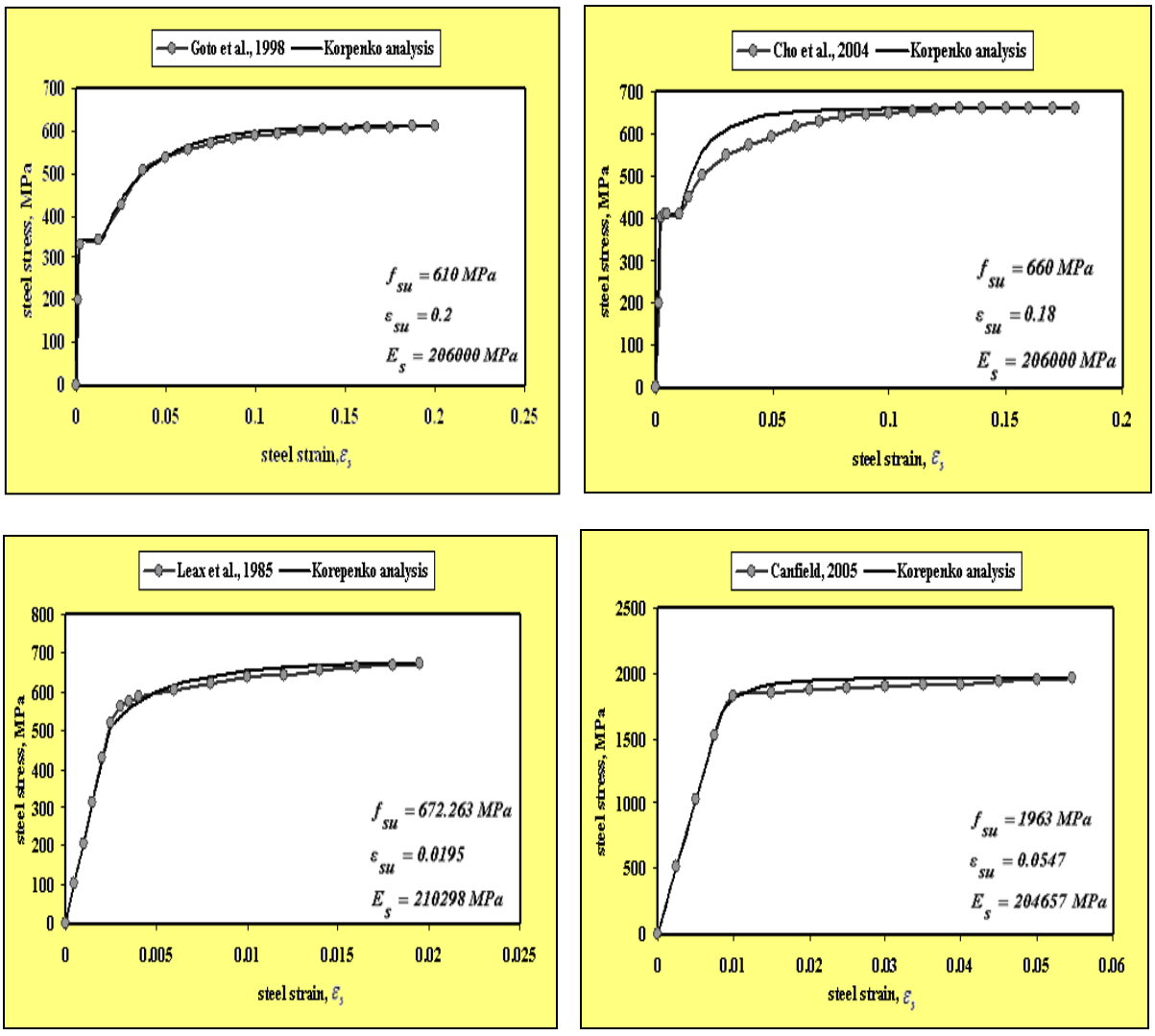

Figure 5: Comparison of proposed model with test data for mild steel and high strength steel

DERIVATION OF ANALYTICAL RELATIONSHIPS TO PREDICT THE LOAD OR MOMENT CAPACITY FOR STRUCTURAL CONCRETE MEMBERS

The analytical model adopts the following assumption (Oukaili, 1998 and Oukaili and Akasha, 2002):

- Cross section is designed to resist the shear and the failure dose not occur because of this effect;
- Linear strain distribution is assumed for across the section depth (Navier law);
- To determine the strain during all load levels until failure, the section between two cracks is assumed;
- The model is based on real stress-strain diagrams for concrete (subjected to tension or compression) and steel;
- Steel and concrete are behaving as nonlinear elastic materials;
- Total stresses are associated with total strains in concrete and steel by secant modulus of elasticity;

In addition to the assumption above it is assumed that (ACI440, 2000)

- The tensile behaviour of the FRP reinforcement is linearly elastic until failure;
- Prefect bond exists between concrete and steel or FRP reinforcement.

The analysis is based on the requirement of equilibrium and compatibility of strain in concrete and steel or FRP. The equilibrium equations take the following form:

$$N = \int_{\Omega_c} \sigma_c \, d\Omega_c + \sum_{i=1}^{m} \sigma_{si} A_{si} + \sum_{i=1}^{n} \sigma_{psi} A_{psi} + \sum_{i=1}^{j} \sigma_{fi} A_{fi}$$

$$M_x = \int_{\Omega_c} \sigma_c y \, d\Omega_c + \sum_{i=1}^{m} \sigma_{si} A_{si} y_{si} + \sum_{i=1}^{n} \sigma_{psi} A_{psi} y_{psi} + \sum_{i=1}^{j} \sigma_{fi} A_{fi} y_{fi} \qquad \textbf{(14)}$$

$$M_y = \int_{\Omega_c} \sigma_c x \, d\Omega_c + \sum_{i=1}^{m} \sigma_{si} A_{si} x_{si} + \sum_{i=1}^{n} \sigma_{psi} A_{psi} x_{psi} + \sum_{i=1}^{j} \sigma_{fi} A_{fi} x_{fi}$$

where:

N: axial force; M_x: bending moment in Y direction; M_y: bending moment in X direction; Ω_c: concrete area; σ_c, σ_{si}, σ_{psi}, σ_{fi}: the stresses in concrete, nonprestressing steel, prestressing steel, and fibre reinforced polymer (FRP), respectively; m, n, j: number of nonprestressing steel, prestressing steel, and FRP, respectively; A_{si}, A_{psi}, A_{fi}: area of nonprestressing steel bars, prestressing steel bars, and FRP elements, respectively (Fig.6); x_{si}, y_{si}, x_{psi}, y_{psi}, x_{fi}, y_{fi}: distance from the centre of gravity of nonprestressing steel, prestressing steel, and FPR to the local coordinate axes, respectively (Fig.7).

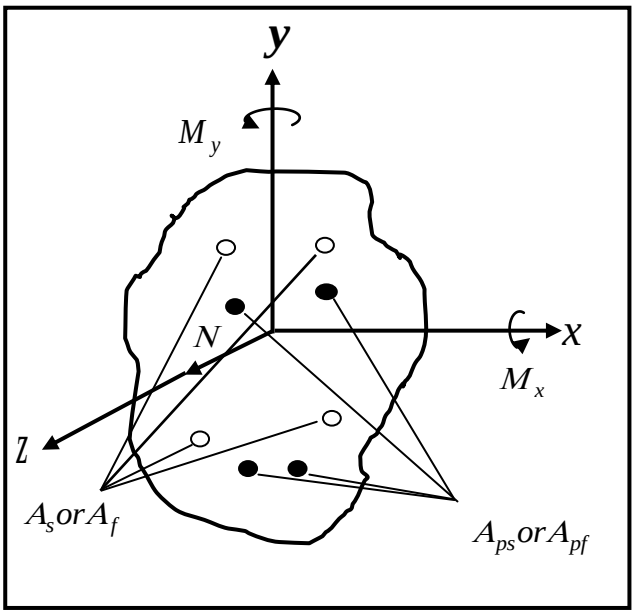

Figure 6: Cross section for member

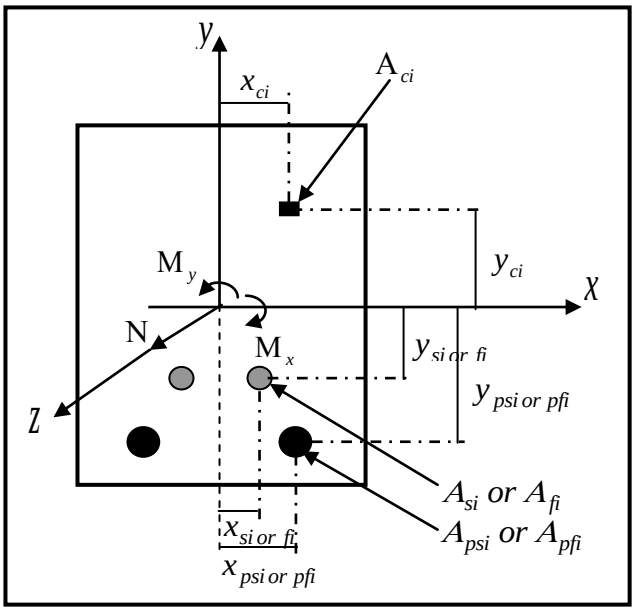

Figure 7: Positive sign for forces on the cross section

The physical relationship is used to determine the stress, which is shown as follows:

$$\sigma = \bar{E}\varepsilon = E\nu\varepsilon \quad \textbf{(15)}$$

where:
$\bar{E}$: secant modulus of elasticity for materials; ν : coefficient of elastic strain.

According to Bernoullis' theory "the plane cross-section before loading remains plane after loading", the strain in any point is expressed as follows (Oukaili, 1998 and Oukaili and Akasha, 2002):

$$\varepsilon = \varepsilon_{om} + \varepsilon_o + K_x y + K_y x \quad \textbf{(16)}$$

where:
ε_{om} : initial strain in materials (concrete , nonprestressed steel, prestressed steel, and FRP) resulted from effective prestressing force, ε_o : strain that result from axial load.
K_x: curvature in Y-direction, K_y: curvature in X-direction, x, y: distance between centre of gravity for concrete, prestressing steel, and nonprestressing steel and the local coordinate axes.

The substitution of Eq.(15) and Eq.(16) in Eq.(14) results in:

$$\begin{Bmatrix} N \\ M_x \\ M_y \end{Bmatrix} = \begin{bmatrix} C_{11} & C_{12} & C_{13} \\ C_{21} & C_{22} & C_{23} \\ C_{31} & C_{32} & C_{33} \end{bmatrix} * \begin{Bmatrix} \varepsilon_o \\ K_x \\ K_y \end{Bmatrix} \quad \textbf{(17)}$$

where:

$$C_{11}=\int_{A_c} E_c\, v_c\, dA_c+\sum_{i=1}^{m} E_{si}\, v_{si}\, A_{si} + \sum_{i=1}^{n} E_{psi}\, v_{psi}\, A_{psi} + \sum_{i=1}^{j} E_{fi}\, A_{fi} \quad (18)$$

$$C_{12}=C_{21}=\int_{A_c} E_c\, v_c\, y_c\, dA_c+\sum_{i=1}^{m} E_{si}\, v_{si}\, A_{si}\, y_{si} + \sum_{i=1}^{n} E_{psi}\, v_{psi}\, A_{psi}\, y_{psi} + \sum_{i=1}^{j} E_{fi}\, A_{fi}\, y_{fi} \quad (19)$$

$$C_{13}=C_{31}=\int_{A_c} E_c\, v_c\, x_c\, dA_c+\sum_{i=1}^{m} E_{si}\, v_{si}\, A_{si}\, x_{si} + \sum_{i=1}^{n} E_{psi}\, v_{psi}\, A_{psi}\, x_{psi} + \sum_{i=1}^{j} E_{fi}\, A_{fi}\, x_{fi} \quad (20)$$

$$C_{22}=\int_{A_c} E_c\, v_c\, y_c^2\, dA_c+\sum_{i=1}^{m} E_{si}\, v_{si}\, A_{si}\, y_{si}^2+\sum_{i=1}^{n} E_{psi}\, v_{psi}\, A_{psi}\, y_{psi}^2 + \sum_{i=1}^{j} E_{fi}\, A_{fi}\, y_{fi}^2 \quad (21)$$

$$C_{23}=C_{32}=\int_{A_c} E_c\, v_c\, x_c\, y_c\, dA_c+\sum_{i=1}^{m} E_{si}\, v_{si}\, A_{si}\, x_{si}\, y_{si} + \sum_{i=1}^{n} E_{psi}\, v_{psi}\, A_{psi}\, x_{psi}\, y_{psi} + \sum_{i=1}^{j} E_{fi}\, A_{fi}\, x_{fi}\, y_{fi} \quad (22)$$

$$C_{33}=\int_{A_c} E_c\, v_c\, x_c^2\, dA_c + \sum_{i=1}^{m} E_{si}\, v_{si}\, A_{si}\, x_{si}^2 + \sum_{i=1}^{n} E_{psi}\, v_{psi}\, A_{psi}\, x_{psi}^2 + \sum_{i=1}^{j} E_{fi}\, A_{fi}\, x_{fi}^2 \quad (23)$$

The direct integration to determine the stiffness matrix elements is not defined mathematically, because secant modulus of elasticity depends on the strain value for material. For that, the numerical integration method is used to determine the stiffness matrix element. In accordance with this model, the member cross section is covered by a mesh with the smallest cells. After that, stress (strain) is determined in each cell and the integral substituted by the process of summation to define the elements of stiffness matrix (Oukaili and Akasha, 2002).

The force vectors equations (Eq.17) have nonlinear behaviour. However in this model, these nonlinear equations are changed to linear equations using the iteration methods with fixity of secant modulus of elasticity in the current iteration cycle (Oukaili, 1998). So that, the stiffness matrix elements take the following form:

$$C_{11}=\sum_{i=1}^{k} E_{ci}\, v_{ci}\, A_{ci}+\sum_{i=1}^{m} E_{si}\, v_{si}\, A_{si}+\sum_{i=1}^{n} E_{psi}\, v_{psi}\, A_{psi} + \sum_{i=1}^{j} E_{fi}\, A_{fi} \quad (24)$$

$$C_{12}=C_{21}=\sum_{i=1}^{k} E_{ci}\, v_{ci}\, A_{ci}\, y_{ci}+\sum_{i=1}^{m} E_{si}\, v_{si}\, A_{si}\, y_{si}+\sum_{i=1}^{n} E_{psi}\, v_{psi}\, A_{psi}\, y_{psi} + \sum_{i=1}^{j} E_{fi}\, A_{fi}\, y_{fi} \quad (25)$$

$$C_{13}=C_{31}=\sum_{i=1}^{k} E_{ci}\, v_{ci}\, A_{ci}\, x_{ci}+\sum_{i=1}^{m} E_{si}\, v_{si}\, A_{si}\, x_{si}+\sum_{i=1}^{n} E_{psi}\, v_{psi}\, A_{psi}\, x_{psi} + \sum_{i=1}^{j} E_{fi}\, A_{fi}\, x_{fi} \quad (26)$$

$$C_{22}=\sum_{i=1}^{k}E_{ci}\,v_{ci}\,A_{ci}\,y_{ci}^{2}+\sum_{i=1}^{m}E_{si}\,v_{si}\,A_{si}\,y_{si}^{2}+\sum_{i=1}^{n}E_{psi}\,v_{psi}\,A_{psi}\,y_{psi}^{2}+\sum_{i=1}^{j}E_{fi}\,A_{fi}\,y_{fi}^{2} \quad (27)$$

$$C_{23}=C_{32}=\sum_{i=1}^{k}E_{ci}\,v_{ci}\,A_{ci}\,x_{ci}\,y_{ci}+\sum_{i=1}^{m}E_{si}\,v_{si}\,A_{si}\,x_{si}\,y_{si}+\sum_{i=1}^{n}E_{psi}\,v_{psi}\,A_{psi}\,x_{psi}\,y_{psi}+\sum_{i=1}^{j}E_{fi}\,A_{fi}\,x_{fi}\,y_{fi} \quad (28)$$

$$C_{33}=\sum_{i=1}^{k}E_{ci}\,v_{ci}\,A_{ci}\,x_{ci}^{2}+\sum_{i=1}^{m}E_{si}\,v_{si}\,A_{si}\,x_{si}^{2}+\sum_{i=1}^{n}E_{psi}\,v_{psi}\,A_{psi}\,x_{psi}^{2}+\sum_{i=1}^{j}E_{fi}\,A_{fi}\,x_{fi}^{2} \quad (29)$$

Where:

C_{11}: axial stiffness, which depends on loading level and geometric properties of the cross section; C_{12}: axial-flexural stiffness, due to axial force (compression or tension) and bending moment in Y-direction, which depends on the geometric properties of cross section, stress-strain condition and the location and direction of selected coordinates axes; C_{13}: axial-flexural stiffness, due to axial force and bending moment in X-direction; C_{22}: flextural stiffness in Y-direction; C_{23}: stiffness, due to bending in X and Y direction, which depends on geometric properties of the section and locations of selected coordinates; C_{33}: flextural stiffness in X-direction; k: number of effective concrete cells; A_{ci}: the cross sectional area of the concrete cell i; x_{ci}, y_{ci}: distance from the centre of gravity of the concrete cell i to the selected coordinates; m: number of nonprestressed longitudinal steel bar in the cross section; A_{si}: the cross sectional area of nonprestressed longitudinal steel bar i;

x_{si}, y_{si}: distance from centre of gravity for nonprestressed longitudinal steel bar i to the selected coordinates; n: number of prestressed longitudinal steel bar in the cross section; A_{psi}: the cross sectional area of prestressed steel bar i; x_{psi}, y_{psi}: distance from the centre of gravity for prestressed longitudinal steel bar i to the selected coordinates; j: number of longitudinal FRP bar in the cross section; A_{fi}: the cross sectional area of the FRP bar i; x_{fi}, y_{fi}: distance from the centre of gravity of longitudinal FRP bar i to the selected coordinates.

The equation (17) can be rewritten in the following shape:

$$\{F\}=[C]^{*}\{\lambda\} \quad (30)$$

Where:

$\{F\}=\lfloor N, M_x, M_y \rfloor$: load vector; $[C]$: section stiffness matrix; $\{\lambda\}=\{\varepsilon_o, K_x, K_y\}^{T}$: axial strain vector.

The stiffness matrix elements depend on the secant modulus of elasticity and the last depends on stress-strain diagrams. Therefore, Eq.(30) takes the following new shape:

$$\{F\}=[C(\varepsilon)]^{*}\{\lambda\} \quad (31)$$

The strain in cross-section determined by Eq.(16). Eq.(31) can take the new shape:

$$\{F\} = [C(\lambda)] * \{\lambda\} \quad \textbf{(32)}$$

In the nonlinear system, Eq.(5-32) represents a compatibility relationship which is used to determine the moment capacity of the structural concrete members.
The analytical model is attributable to using discrete approaches and nonlinear analysis using modern electronic computers and using numerical methods (Oukaili and Akasha, 2002*)*. Oukaili program (Oukaili, 1999) called SECTION is used in this paper.

6. Structural Concrete Members Reinforced with Fibre Reinforced Polymer (FRP) Bars

Simply supported beams for other investigators are examined to study the flexural behaviour of the structural concrete members reinforced with FRP bars. These beams are shown as follows:

6.1 Aiello and Ombres (2000)

Aiello and Ombres (2000) cast nine concrete beams reinforced with AFRP rebars for flexural tests to examine the failure load. The tensile reinforcement area is 176.7mm^2. The beam spanning 2610 mm was subjected to four-point bending. The cross sectional geometry and test set-up beam are as shown in Fig.8.

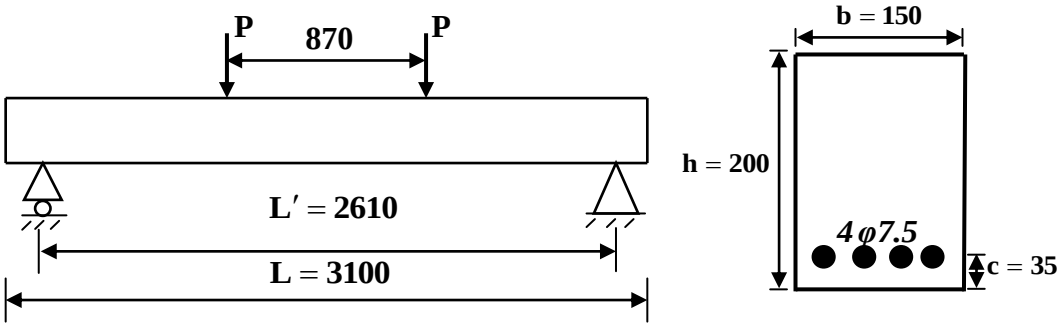

all dimension in mm

Figure 8: Cross section and test set-up of beam A

Average value of the tensile strength and modulus of elasticity of the rebars determined by standard tensile test, are 1506 and 50100 MPa, respectively. The average compressive strength of the concrete is 46.2 MPa. ACI 318 Committee (ACI 318, 2008) expression is used to determine the modulus of rupture and modulus of elasticity and shown as follows:

$$f_r = 0.62\sqrt{f'_c} \quad \textbf{(33)}$$

$$E_c = 4730\sqrt{f'_c} \quad \textbf{(34)}$$

To determine the strain corresponding to the maximum stress ε_o the empirical equation assumed by Smith and Young (Smith and Young, 1956) is used and shown as follows:

$$\varepsilon_0 = (0.71\ f'_c + 168) \times 10^{-5} \quad \textbf{(35)}$$

For that, the compressive strain ε_o, modulus of rupture and modulus of elasticity for concrete are 0.002, 4.214 and 32286 MPa, respectively.

The analytical moment-curvature relationship at critical section is evaluated for beam A, which is shown in Fig.9.

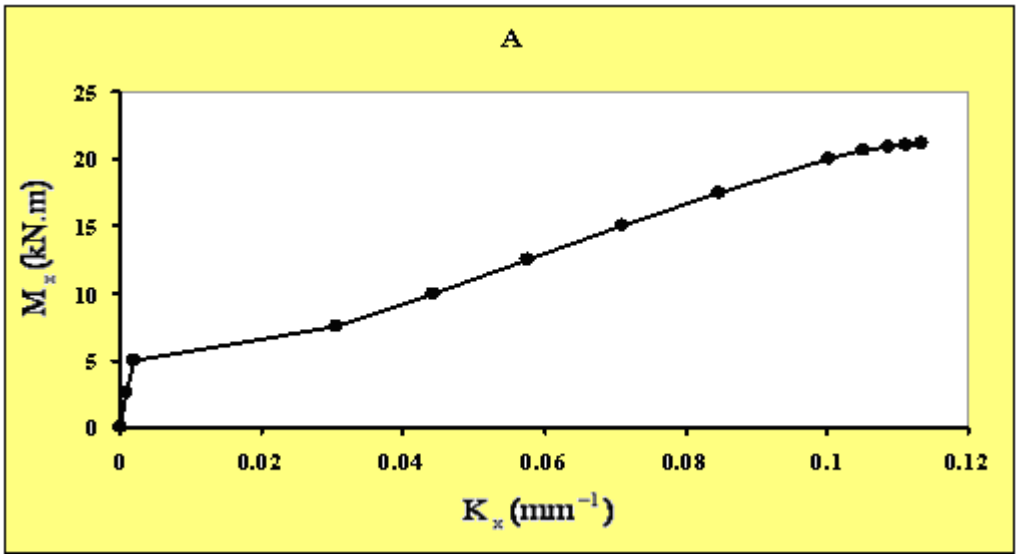

Figure 9: Theoretical moment-curvature diagram for beams A

Beam A failed experimentally at a bending moment of 22.84 kN.m. Analytical moment capacity is determined based on the used model in this study and the model recommended by ACI 440H Committee; these moments are 21.17 kN.m and 19.062 kN.m, respectively.

Dolan and Burke (2001)

Two rectangular and T-section beams reinforced with prestressed CFRP bar were tested by Dolan and Burke (2001). Beam strawman 3 is studied in this section. This beam is simply supported and was subjected to four-point flexural testing. The cross section dimension and flexural testing of beam is shown in Fig.10.

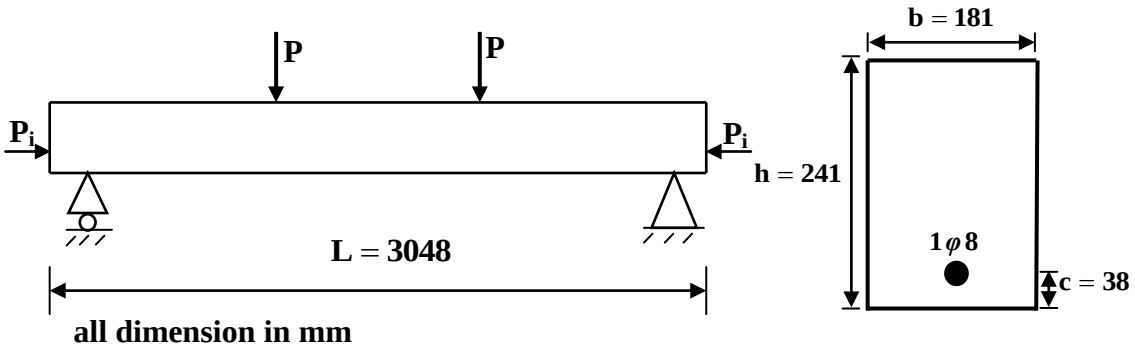

Figure 10: Cross section dimension and flexural testing for strawman 3

The measure compressive strength of concrete used in the beam is 31 MPa. The other mechanical properties of concrete are determined using the same empirical equation in section 6. 1.

Therefore, the calculated value of the compressive strain ε_o, modulus of rupture and modulus of elasticity is 0.0019, 3.452, 26336 MPa, respectively. The mean tensile strength of FRP is 1862 MPa, and the mean modulus of elasticity for the CFRP bars is 146 GPa. The tensile reinforcement area is 50.3 mm^2 and the initial prestressing force is 53.4 kN.

The analytical moment-curvature diagram for Strawman 3 beam is shown in Fig.11.

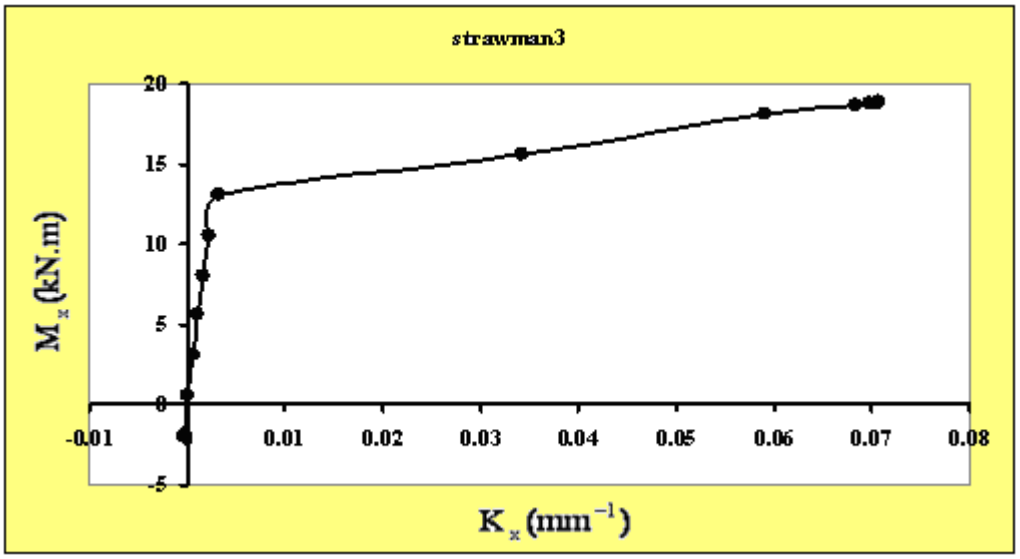

Figure 11: Theoretical moment-curvature diagram for beam strawman 3

Strawman 3 beam is failed experimentally at moment 19.1 kN.m, while the moment from the used model and Burke and Dolan is 18.856 and 18.293 kN.m, respectively.

STRUCTURAL CONCRETE MEMBERS REINFORCED WITH FIBRE REINFORCED POLYMER (FRP) PLATE

External reinforcement with nonprestressed and prestressed FRP plate for simply supported concrete beams under flextural test for many investigators are used in this study. Detailed study for some beams is shown as follows:

Nguyen et al. (2001)

Simply supported beams strengthened with CFRP plate were studied by Nguyen et al. 2001. A1500 beam has 120 × 150 mm cross section and 1500 mm length, this beam is subjected to four point loads. Detail of the beam and test loading is shown in Fig.12.

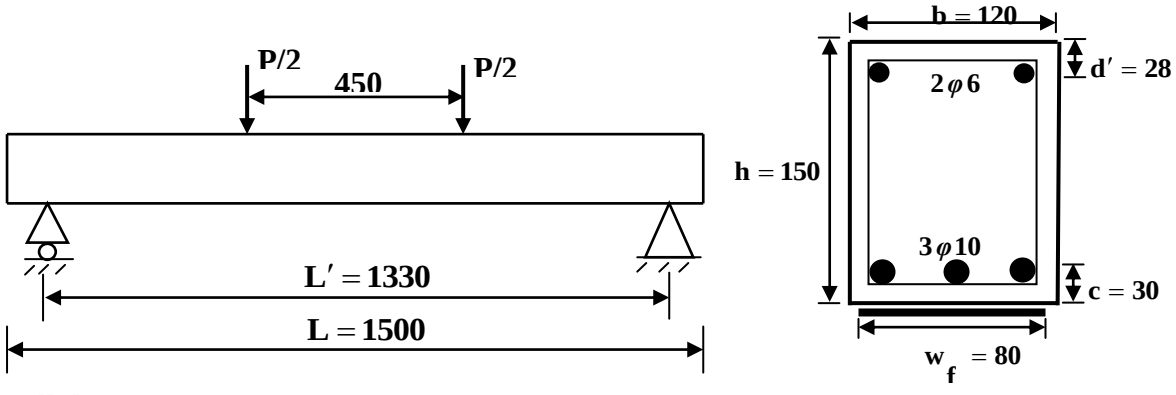

The tension and compression reinforcement areas of the beam are 236 and 56.5 mm^2. The CFRP plate of 80 × 1.2 mm cross section is used. The compressive strength of concrete is 44.6 MPa. Table (1) presents the mechanical properties for materials.

Table (1): Mechanical properties of materials

Materials	Reinf. Area mm^2	Yield Strength MPa	Ultimate Strength Mpa	Modulus of Rupture MPa	Modulus of Elasticity GPa	Ultimate Strain	Strain at Maximum Stress
CFRP plate	*96*	-	*3140*	-	*181*	-	-
Tension reinforcement bar	*236*	*384*	*461**	-	*200**	*0.17**	-
Compression reinforcement bar	*56.2*	*400*	*480**	-	*200**	*0.17**	-
Concrete	-	-	*44.6*	*4.141*†	*31.588*†	-	*0.002*†

†*assumed* ($f_r = 0.62\sqrt{f'_c}$, $\varepsilon_0 = (0.71\ f'_c + 168)\times 10^{-5}$, $E_c = 4730\sqrt{f'_c}$) * *assumed*

The moment-curvature of this beam is shown in Fig.13.

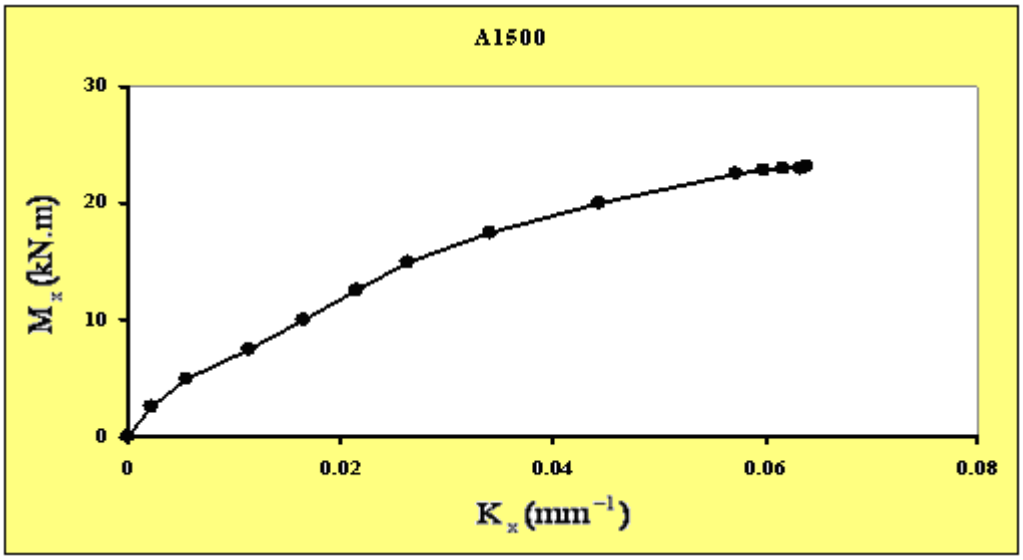

Figure 13: Theoretical moment-curvature diagram for beam A1500

The beam A1500 failed at the experimental applied moment of 25.96 kN.m. While, the ultimate moment from the used model and ACI 440H Committee is 23.066 and 18.311 kN.m, respectively.

Zou et al. (2005)

Zou et al., (2005) has studied the flexural behaviour of five reinforced concrete beams strengthened by prestressed CFRP. Three of these beams are used in this study. All beams have the

same dimension of 100 × 150 × 2200 mm (width × depth × length). The clear span 2000 mm of the beams have been loaded by two equal forces. The cross section dimension and test of set-up are shown in Fig.14.

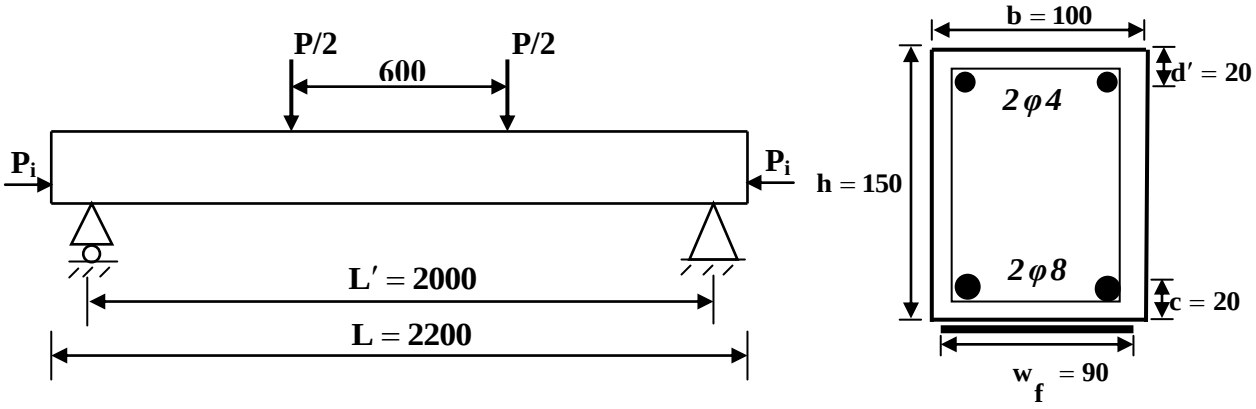

Figure 14: Cross section dimensions and flexural testing

The average compressive strength of concrete is 19.92 MPa for three specimens. The area of CFRP sheet used is 90 mm wide with an average thickness of 0.167 mm and the initial prestressing force is 22 kN. Table (2) shows details of mechanical properties for materials.

Table (2): Mechanical properties for materials

Materials	Reinf. Area mm^2	Yield Strength MPa	Ultimate Strength MPa	Modulus of Rupture MPa	Modulus of Elasticity GPa	Ultimate Strain	Strain at Maximum Stress
CFRP plate	*15.03*	-	*2941*	-	*207.2*	-	-
Tension reinforcement bar	*101*	*309.9*	*372**	-	*224.5*	*0.17**	-
Compression reinforcement bar	*25*	*595*	*714**	-	*201.2*	*0.2**	-
Concrete	-	-	*19.92*	*2.767†*	*21111†*	-	*0.00182†*

*†assumed ($f_r = 0.62\sqrt{f'_c}$, $\varepsilon_0 = (0.71\ f'_c + 168)\times 10^{-5}$, $E_c = 4730\sqrt{f'_c}$), * assumed*

Fig. 15 shows the moment curvature diagram for beam B5.

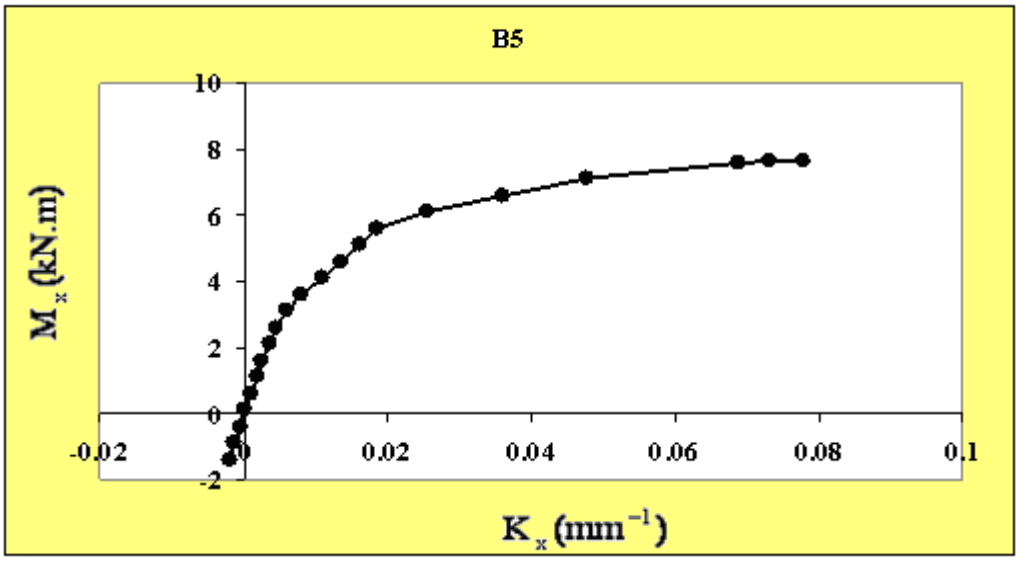

Figure 15: Moment-curvature diagrams for prestressed beam B5

Beam B5 has failed at moment 8.75 kN.m, while the ultimate analytical moment is 7.647 kN.m.

CONCLUSIONS

- The modelling of materials presented in this study is good to represent the actual stress-strain diagrams of LSC, NSC and HSC and mild and high strength steel.
- The presented model gives good agreement with experimental results for the structural concrete member reinforced with nonprestressed FRP bar and plate.
- A reasonable agreement between the analytical and experimental results of the structural concrete member reinforced with external FRP plate is observed.

REFERENCE

- ACI Committee 318, 2008, ***Building Code Requirements for Structural Concrete***, American Concrete Institute, Detroit (MI).
- ACI Committee 440H, 2000***, Guide for Design and Construction of Concrete Reinforced with FRP Bars***, American Concrete Institute, Detroit, Mich., pp.1-97.
- Aiello, M.; and Ombres, L.; 2000, ***Load-Deflection Analysis of FRP Reinforced Concrete Flexural Members***, Journal of Composites for Construction, Vol.4, No.4, pp.164-171.
- Canfield, S.R.; 2005, ***Full Scale Testing of Prestressed, High Performance Concrete, Composite Bridge Girders***, M.Sc.Thesis, Georgia Institute of Technology, The Academic Faculty.
- Cho, J.; Kim, N.; Cho, N.; and Choi, I.; 2004, ***Cracking Behaviour of Reinforced Concrete Panel Subjected to Biaxial Tension***, ACI Structural Journal, Vol.101, No.1, pp.76-84.

- Goto, Y.; Wang, Q.; and Obata, M.; 1998, ***FEM Analysis for Hysteretic Behaviour of Thin-Walled Columns***, Journal of Structural Engineering, Vol.124, No.11, pp.1290-1301.

- Dolan, C.W.; Rizkalla, S.; and Nanni, A.; 1999, ***Fibre-Reinforced-Polymer Reinforcement for Reinforced Concrete Structure, SP-188***, American Concrete Institute, Farmington Hills, MI, pp.1182.

- Dolan, C.; and Burke, C.R.; 2001, ***Flexural Design of Prestressed Concrete Beams Using FRP Tendons***, PCI Journal, Vol.46, No.2, pp.76-87.

- Korpenko, N.I.; Mukhamediev, T.A.; and Petrov, A.N.; 1986, ***The Initial and Transformed Stress-Strain Diagrams of Steel and Concrete***, Special Publication, Stress–Strain Condition for Reinforced Concrete Construction, Reinforced Concrete Research Centre, Moscow, pp.7-25.

- Leax, T.R.; Dowling, N.E.; Brose, W.R.; and Peck, M.G.; 1985, ***Methodology for Correlating Fatigue Data Obtained under Different Test Conditions***, Journal for Testing and Evaluation, JTEVA, Vol.13, No.6, pp.393-404.

- Nguyen, D.M.; Chan, T.K.; and Cheong, H.K.; 2001, ***Brittle Failure and Bonded Development Length of CFRP-Concrete Beams***, Journal of Composite for Construction, Vol.5, No.1, pp.12-17.

- Nilson, A.H.; Slate, F.O.; and Martinez, S.; 1986, ***Mechanical Properties of High-Strength Light Weight Concrete***, ACI Journal Proceeding, Vol.83, No.4, pp.606-613.

- Oukaili, N.K.; 1998, ***Moment Capacity and Strength of Reinforced Concrete Members Using Stress-Strain Diagrams of Concrete and Steel***, Journal King Saud Univ., V.10, No.2, pp.23-44 (in Arabic).

- Oukaili, N.K.; 1999, ***Model for Predicting the Cracking Moment in Structural Concrete Members***, Al-Yarmok Searches (Sciences Series of Essential and Engineering), V.8, No.2, pp.9-39 (in Arabic).

- Oukaili, N.K.; and Akasha, A.M.; 2002, ***General Program to Study the Behaviour of Concrete Structural under Static Loads***, First Civil Engineering Conference, Sebha University, (Sebha, Liyba), pp.1-19, (in Arabic).

- **Pešić**, N.; and Pilakoutas, K.; 2005, ***Flexural analysis and design of reinforced concrete beams with externally bonded FRP reinforcement***, Materials and Structures, Vol.38, pp.183-192.

- Smith, G.M.; and Young, L.E.; 1956, ***Ultimate Flexural Analysis Based on Stress-Strain Curves of Cylinders***, ACI Journal, Proceedings, V.53, No.6, pp.597-609.

- Tasnimi, A.A.; 2004, ***Mathematical Model for Complete Stress-Strain Curve Prediction of Normal, Light-Weight and High-Strength Concretes***, Magazine of Concrete Research, Vol.56, No.1, February, pp.23-34.

- Wang, P.T.; Shah, S.P.; and Naaman, A.E.; 1978, ***Stress-Strain Curve for Normal and Light Weight Concrete in Compression***, ACI Journal Proceeding, Vol.75, No.11, pp.603-611.

- Zou, P.; Shang, S.; Peng, H.; and Wang, H.; 2005, ***Avoiding De-bonding in FRP Strengthened Reinforced Concrete Beams Using Prestressing Techniques***, Proceeding of The International Symposium on Bond Behaviour of FRP in Structure (BBFS) Chen and Teng (eds).